Scientia Iranica A (2012) 19 (6), 1411–1421

Sharif University of Technology

Scientia Iranica

Transactions A: Civil Engineering

www.sciencedirect.com

Bearing failure modes of rock foundations with consideration of joint spacing

M. Imani [a], A. Fahimifar [a,*], M. Sharifzadeh [b]

[a] *Department of Civil and Environmental Engineering, Amirkabir University of Technology, Tehran, Iran*
[b] *Department of Mining and Metallurgy Engineering, Amirkabir University of Technology, Tehran, Iran*

Received 18 October 2011; revised 29 June 2012; accepted 7 August 2012

KEYWORDS
Jointed rock foundation;
Bearing capacity;
General shear failure;
Excessive deformation;
Joint spacing.

Abstract In this study, two main failure modes of jointed rock foundations consisting general shear failure and failure due to excessive deformation are discussed. For each of these two modes, the method of determining ultimate bearing capacity is presented and the effect of joint spacing is also examined. For the former mode, an upper bound method of limit analysis is employed, while for the latter one, distinct element numerical modeling is used to investigate the effect of joint spacing on the bearing capacity. The calculations are performed for a rock mass containing two orthogonal joint sets that the orientation angle of the first joint set is 15°, 30° and 45° to the horizontal, respectively. A non-dimensional parameter called "Spacing Ratio" (*SR*) is used to examine the effect of different joint spacing. This study shows that in the case of general shear failure mode, joint spacing does not have significant effect on the bearing capacity. In the failure mode induced by excessive deformation of the rock mass, for $SR < 30$, increasing the *SR* results in decreasing the bearing capacity, however, for $SR > 30$, the joint spacing does not significantly affect the bearing capacity.

1. Introduction

The bearing capacity of a strip footing resting on soil has been widely studied in the literature. Because of inhomogeneity and discontinuity of rock masses, few attempts have been made to study the bearing capacity of rock foundations, particularly jointed rocks. Among them, the researches performed by Serrano and Olalla [1,2], Sutcliffe et al. [3], Yang and Yin [4], Merifield et al. [5] and Saada et al. [6] are concerned with rock masses obeying Hoek–Brown failure criterion which is applicable for intact or heavily crushed rocks. Moreover, using the upper bound method of limit analysis, Maghous et al. [7] assessed the load bearing capacity of rock foundations resting on a regularly jointed rock. They considered the rock matrix and the joints separately, and compared the obtained results by those derived through considering the jointed rock mass as a homogenized medium. Sutcliffe et al. [3] analyzed the bearing capacity of rock masses containing one to three sets of closely spaced joints. Also, Halakatevakis and Sofianos [8] analyzed a series of jointed rock samples containing one to three joint sets with various spacing and dip angles using the distinct element code, UDEC. They have concluded that the strength of the models is independent of the joint spacing. No further published documents regarding the effects of joint spacing on the bearing capacity of rock foundations have been found.

Depending on the failure mode of rock foundations, spacing of joints has different influences on the bearing capacity. In practice, two main failure modes may occur which are named as general shear failure and punching shear failure. The latter can be attributed as the failure due to excessive deformation. Most of the above mentioned methods for determining rock bearing capacities are based on the general shear failure mode.

In this paper, the two mentioned failure modes are discussed precisely for a rock mass containing two orthogonal joint sets. The effect of joint spacing on the bearing capacity of rock foundations in each of these failure modes is also investigated. For the general shear mode, an upper bound method of limit analysis is employed and the ultimate bearing capacity

* Corresponding author. Tel.: +98 2164543011; fax: +98 2164543011.
E-mail address: Fahim@aut.ac.ir (A. Fahimifar).

Peer review under responsibility of Sharif University of Technology.

Production and hosting by Elsevier

doi:10.1016/j.scient.2012.10.007

Nomenclature

B	foundation width
c_i	cohesion of intact rock
c_j	cohesion of joint set
D	total energy dissipation
DEM	distinct Element Method
K_n	joint normal stiffness
K_s	joint shear stiffness
n	joint sets number
n_0	an integer number
N_{cj}, N_{ci}, N_q and N_γ	bearing capacity coefficients
q	surcharge
q_u	ultimate bearing capacity of dry rock
SR	spacing ratio
S_i	spacing of the ith joint set
UBS	upper bound solution proposed in this study
W	total work of external forces
α	orientation angle of one of the joint sets with horizontal direction
γ	unit weight of rock mass
θ	angle between the velocity discontinuity line passing through intact rock with horizontal direction
φ_i	friction angle of intact rock
φ_j	friction angle of joint set

equation is derived in which the joint spacing can be taken into account. Orientation angles equal to 15°, 30° and 45° were selected for one of the joint sets, while the second joint set was assumed to be perpendicular to the first set. For the failure mode, due to excessive deformation, Distinct Element Method (DEM) was used to investigate the effect of joint spacing on the bearing capacity. In this regard, the concept of "spacing ratio" (SR) initially proposed by Serrano and Olalla [9] was used to introduce joint spacing into the discontinuum numerical models. The non-dimensional parameter, SR, is expressed as follows:

$$SR = B \sum_{i=1}^{n} \frac{1}{S_i}, \tag{1}$$

where, B is the footing width, S_i is the spacing of the ith joint set and n is the number of joint sets.

Using load–settlement curve obtained from the numerical analyses, the ultimate bearing capacity was obtained for different SRs; and the particular SR, in which the rate of variation of the bearing capacity becomes negligible, was selected as the limit of joint spacing effectiveness. This limiting value is called as the critical spacing ratio (SR_{cr}). Finally, a procedure for determining allowable bearing capacity of rock masses was proposed in this paper which can be used in practical applications.

2. Modes of bearing failure of rock foundations

In the case of general shear failure, a continuous shear failure occurs in the rock bedding from beneath the footing to the ground surface and results in pushing up the bedding on both sides of the footing. But in failure, due to excessive deformation (punching shear failure), the failure takes place beneath the footing and the rock mass outside the loaded area remains relatively uninvolved, so the movement on both sides of the footing will be minimal. In the case of soil beddings, latter type of failure is typically observed in compressible soils. The failure due to excessive deformation may also take place in rock masses but often not as a result of compressibility of the mass, because even weak rock masses are not as compressible as most types of soils. As emphasized by Eurocode 7 [10], one of the different types of limit states for a rock foundation is the excessive deformation of the ground in which the strength of rock is significant. In such a case, the mobilized bearing pressure continuously increases with the footing movement, apparently without reaching an ultimate bearing capacity, at least within the bounds of small displacement approach. Therefore, the slip surfaces do not reach the ground surface and a large settlement occurs in the rock mass. In this case, the methods of determining the bearing capacity based on the general shear failure may not accurately result in the critical load. A proper approach for determining the critical load in such cases is to use the load–settlement curve of the rock foundation.

In practical situations, depending on the rock mass properties, the failure due to excessive deformation may occur prior to the general shear failure which reveals the necessity of taking care of deformations. In the following sections, the procedure used for determining ultimate bearing capacity in each of the two mentioned failure modes is investigated and the effect of joint spacing is discussed.

2.1. General shear failure

Upper bound theorem of limit analysis was applied to obtain the bearing capacity of a rock mass subjected to the general shear failure. According to the theorem, the rate of energy dissipation is not less than the rate of work of the external forces for any kinematically admissible failure mechanism.

Construction of an admissible failure mechanism is the first step in solving the bearing capacity problem using the upper bound method. In the foundations with centric and vertical loadings, the failure mechanism is usually considered to be symmetrical (i.e. a two-sided mechanism). However, in jointed rock masses, the failure mechanism may be affected by the joint sets, and thus converted to an asymmetrical shape. For determining the shape of the failure mechanism, numerical analyses were performed using the distinct element code, UDEC. Since the upper bound formulation obtained here is valid only for the case of general shear failure, the properties of intact rock and joint sets were selected such that the failure surfaces in the rock mass reach the ground surface (general shear failure).

The numerical modeling was performed for a flexible foundation with one meter width located on the surface of a jointed rock mass containing two orthogonal joint sets in which orientation angles equal to $\alpha = 15°$, 30° and 45° were considered for one of the joint sets. It was assumed that the joints are starting from the foundation extremities. In the analyses, different SR values, at the range of 3–50, were examined. The rock blocks were assumed to be deformable and Mohr Coulomb failure criterion was used for the rock material and the joint sets.

As an example, for the intact rock cohesion (c_i) equal to 5 MPa, joint sets cohesion (c_j) equal to 50 kPa and intact rock and joint sets friction angles (φ_i and φ_j, respectively) equal to 35°, the displacement vectors of the rock blocks are shown in the left hand side of Figure 1. For $\alpha = 45°$, the mechanism is symmetrical (a two-sided mechanism), while for

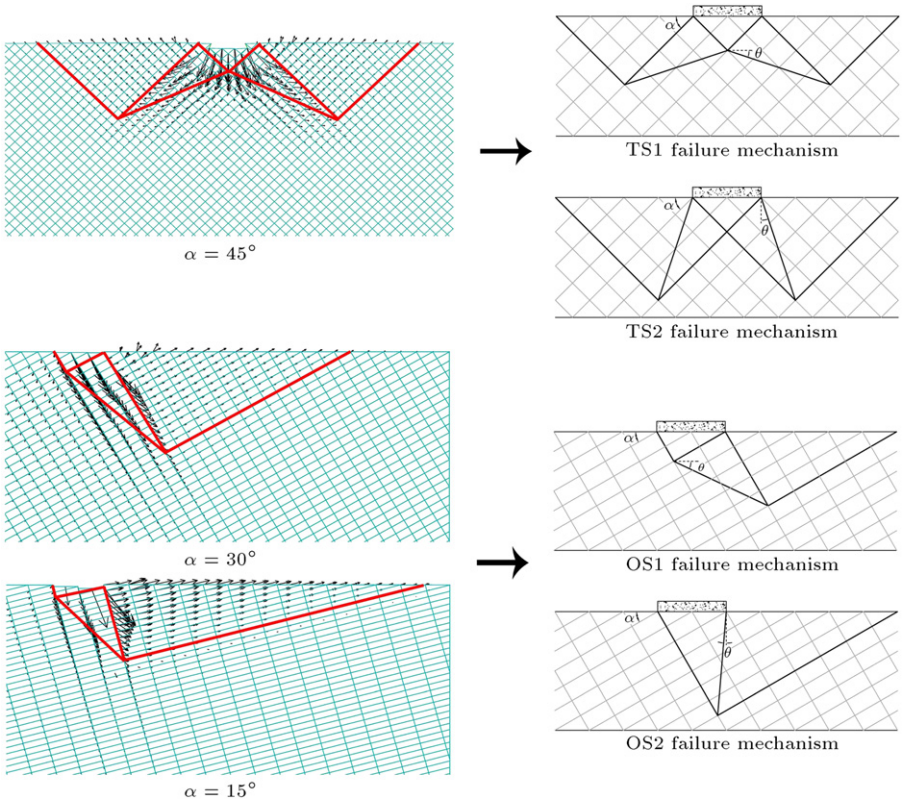

Figure 1: Displacement vectors obtained using distinct element method for the case of $SR = 10$ and the overall shape of the failure mechanisms.

$\alpha = 30^\circ$ and 15°, the mechanism is asymmetrical (a one-sided mechanism). Moreover, keeping the above-mentioned properties unchanged, the effect of joint spacing on the configuration of failure mechanism was also investigated and no remarkable effect of joint spacing on the shape of the failure mechanism was observed. Hence, a two-sided symmetrical failure mechanism (TS failure mechanism) was used for the case of $\alpha = 45^\circ$ and a one-sided asymmetrical failure mechanism (OS failure mechanism) was used for $\alpha = 15^\circ$ and 30°. For obtaining the least magnitude of upper bound bearing capacity, two different TS mechanisms (named TS1 and TS2) and also two different OS mechanisms (named OS1 and OS2) were considered as shown in the right hand side of Figure 1.

2.1.1. Failure mechanisms TS1 and OS1

The mechanisms TS1 and OS1 and the corresponding hodographs are shown in Figure 2. In order to minimize the maximum internal energy dissipation, and thus to obtain minimum values for the upper bound bearing capacity, the greatest possible length of velocity discontinuity lines have been passed along the joints. It is assumed that both the beginning and the end points of line CD are located at the junction of the two joint sets, not within the intact rock block. For satisfaction of this assumption, CD was considered as a straight line. In the case of assuming a logarithmic-spiral curve for CD (such as the one considered in Prandtl mechanism), it is possible that point D does not locate at the junction of the two joint sets.

For TS1, since the movements are symmetrical about the footing vertical axis, it is enough to consider the movement through the half of the mechanism.

Rock masses may not obey the associated flow rule. However, in a large number of stability problems such as bearing capacity, deformation conditions are not so restrictive and the rock deformation properties do not greatly affect the collapse load. Therefore, the adoption of the associated flow rule appears to be reasonable in the limit analysis [11]. According to the normality rule, the velocity on every discontinuity line must be inclined at an angle φ with that line, where φ is the friction angle of the medium in which the discontinuity line lays (either φ_i or φ_j). All the velocities of the mechanism determined in this way, constitute a kinematically admissible velocity field.

In Figure 2, the foundation width (B), the spacing of the joints (S_1), α, φ_i and φ_j are known. Since the absolute magnitude of the velocity has no influence on the final results, it is assumed that the magnitude of V_0 is equal to unity, i.e. $V_0 = 1$. From the geometrical relations in the hodographs shown in Figure 2, the magnitudes of other velocity vectors can be calculated as follows:

For the mechanism TS1, see Box I.

For the mechanism OS1, see Box II.

The angle of line CD with the horizontal direction (θ) is:

$$\theta = \tan^{-1}\left(\frac{n_0 S_1}{B\cos\alpha}\right) - \alpha, \tag{10}$$

where n_0 is an integer number which by being multiplied by S_1, the length of velocity discontinuity line BD is obtained. So, the only unknown parameter of the failure mechanisms is n_0.

The rate of energy dissipation (D_L) along each velocity discontinuity line is:

$$D_L = c \cdot V \cdot \cos\phi, \tag{11}$$

where c is the cohesion (either c_i or c_j), and V is the velocity magnitude that makes the angle φ_i or φ_j with a velocity

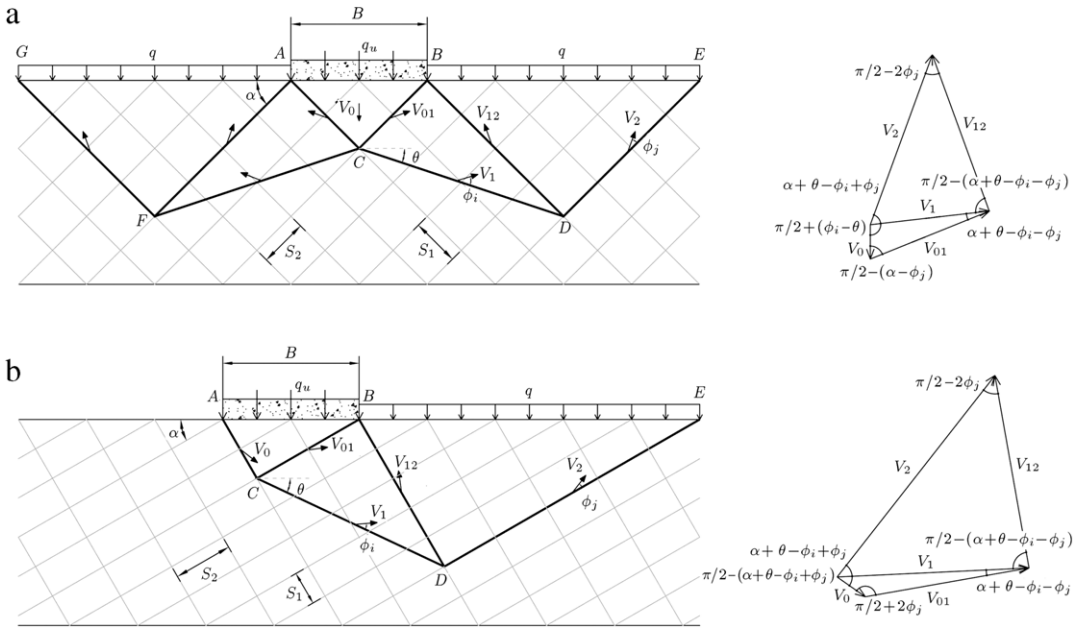

Figure 2: Failure mechanisms and the corresponding hodographs (a) TS1 and (b) OS1.

$$V_{01} = V_0 \cdot \frac{\cos^2(\phi_i - \theta)}{\sin(\alpha - \phi_j) - \sin(\phi_i - \theta) \cdot \cos(\alpha + \theta - \phi_i - \phi_j)}, \tag{2}$$

$$V_1 = V_0 \cdot \frac{-\sin(\alpha - \phi_j) \cdot \sin(\phi_i - \theta) + \cos(\alpha + \theta - \phi_i - \phi_j)}{\sin(\alpha - \phi_j) - \sin(\phi_i - \theta) \cdot \cos(\alpha + \theta - \phi_i - \phi_j)}, \tag{3}$$

$$V_{12} = V_1 \cdot \frac{\sin^2(\alpha + \theta - \phi_i + \phi_j)}{\sin(2\phi_j) \cdot \cos(\alpha + \theta - \phi_i + \phi_j) + \sin(\alpha + \theta - \phi_i - \phi_j)}, \tag{4}$$

$$V_2 = V_1 \cdot \frac{\sin(2\phi_j) + \cos(\alpha + \theta - \phi_i + \phi_j) \cdot \sin(\alpha + \theta - \phi_i - \phi_j)}{\sin(2\phi_j) \cdot \cos(\alpha + \theta - \phi_i + \phi_j) + \sin(\alpha + \theta - \phi_i - \phi_j)}. \tag{5}$$

Box I

$$V_{01} = V_0 \cdot \frac{\cos^2(\alpha + \theta - \phi_i + \phi_j)}{\cos(\alpha + \theta - \phi_i - \phi_j) \cdot \sin(\alpha + \theta - \phi_i + \phi_j) - \sin(2\phi_j)}, \tag{6}$$

$$V_1 = V_0 \cdot \frac{\cos(\alpha + \theta - \phi_i - \phi_j) - \sin(\alpha + \theta - \phi_i + \phi_j) \cdot \sin(2\phi_j)}{\cos(\alpha + \theta - \phi_i - \phi_j) \cdot \sin(\alpha + \theta - \phi_i + \phi_j) - \sin(2\phi_j)}, \tag{7}$$

$$V_{12} = V_1 \cdot \frac{\sin^2(\alpha + \theta - \phi_i + \phi_j)}{\sin(2\phi_j) \cdot \cos(\alpha + \theta - \phi_i + \phi_j) + \sin(\alpha + \theta - \phi_i - \phi_j)}, \tag{8}$$

$$V_2 = V_1 \cdot \frac{\sin(2\phi_j) + \cos(\alpha + \theta - \phi_i + \phi_j) \cdot \sin(\alpha + \theta - \phi_i - \phi_j)}{\sin(2\phi_j) \cdot \cos(\alpha + \theta - \phi_i + \phi_j) + \sin(\alpha + \theta - \phi_i - \phi_j)}. \tag{9}$$

Box II

discontinuity line. Thus, the total energy dissipation (D) in the mechanism TS1 is:

$$D = 2 \times (D_{BC} + D_{CD} + D_{BD} + D_{DE}). \tag{12}$$

In the mechanism OS1 it changes to:

$$D = D_{AC} + D_{BC} + D_{CD} + D_{BD} + D_{DE}, \tag{13}$$

where D_{XY} is the energy dissipation along the discontinuity line, XY.

The total external work (W) in the mechanism TS1 is:

$$W = W_{ABC} + 2 \times \left(W_{BCD} + W_{BDE} + W_q\right) + W_{q_u}. \tag{14}$$

And, in the mechanism OS1 it changes to:

$$W = W_{ABC} + W_{BCD} + W_{BDE} + W_q + W_{q_u}, \tag{15}$$

where W_{XYZ} is the external work of wedge XYZ, W_q is the external work of surcharge q and W_{qu} is the external work of

foundation load which are as follows for TS1 and OS1:

$$W_{q_u,(\mathrm{TS1})} = q_u \cdot B \cdot V_0, \tag{16}$$

$$W_{q_u,(\mathrm{OS1})} = q_u \cdot B \cdot V_0 \cdot \cos\left(\alpha + \phi_j\right). \tag{17}$$

For TS1, by equating Eqs. (12) and (14) and using Eq. (16), the ultimate bearing capacity for TS1 was obtained as in Box III.

For OS1, by equating Eqs. (13) and (15) and using Eq. (17), the ultimate bearing capacity for OS1 was obtained as in Box IV.

Finally, after some rearrangements, the general equation for the upper bound of ultimate bearing capacity (q_u) of a shallow foundation on the assumed jointed rock is obtained as:

$$q_u = c_j N_{cj} + c_i N_{ci} + q N_q + \frac{1}{2}\gamma B N_\gamma, \tag{20}$$

where γ is the total unit weight of the rock mass, N_{cj}, N_{ci}, N_q and N_γ are the bearing capacity coefficients that are as follows for TS1 and OS1. Assuming:

$$\xi_1 = \alpha + \theta - \phi_i - \phi_j, \tag{21}$$

$$\xi_2 = \alpha + \theta - \phi_i + \phi_j, \tag{22}$$

$$\xi_3 = \alpha + \phi_j, \tag{23}$$

$$\xi_4 = \alpha + \theta, \tag{24}$$

$$\xi_5 = \phi_i - \theta, \tag{25}$$

$$\xi_6 = \alpha - \phi_j. \tag{26}$$

For the mechanism TS1:

$$N_{cj} = \frac{2\cos\phi_j \cos\alpha}{f_1} \times \left[\cos^2\xi_5 + \frac{f_2}{f_3}\cdot\tan\xi_4\left(\sin^2\xi_2 + \frac{f_4}{\tan\alpha}\right)\right], \tag{27}$$

$$N_{ci} = \frac{f_2}{f_1}\cdot\frac{2\cos\phi_i\cos\alpha}{\cos\xi_4}, \tag{28}$$

$$N_q = \frac{f_2 f_4}{f_1 f_3}\cdot\frac{2\sin\xi_3\tan\xi_4}{\tan\alpha}, \tag{29}$$

$$N_\gamma = \cos\alpha\left[\frac{2f_2}{f_1}\cdot\cos\alpha\tan\xi_4 \times \left(\sin\xi_5 + \frac{f_4}{f_3}\cdot\frac{\sin\xi_3\tan\xi_4}{\tan\alpha}\right) - \sin\alpha\right], \tag{30}$$

where:

$$f_1 = \sin\xi_6 - \sin\xi_5\cos\xi_1, \tag{31}$$

$$f_2 = -\sin\xi_6\sin\xi_5 + \cos\xi_1, \tag{32}$$

$$f_3 = \sin 2\phi_j\cos\xi_2 + \sin\xi_1, \tag{33}$$

$$f_4 = \sin 2\phi_j + \cos\xi_2\sin\xi_1. \tag{34}$$

For the mechanism OS1:

$$N_{cj} = \frac{\cos\phi_j\cos\alpha}{\cos\xi_3}\left[\tan\alpha + \frac{\cos^2\xi_2}{g_1} + \frac{g_2}{g_1 g_3}\cdot\tan\xi_4\left(\sin^2\xi_2 + \frac{g_4}{\tan\alpha}\right)\right], \tag{35}$$

$$N_{ci} = \frac{g_2}{g_1}\cdot\frac{\cos\phi_i\cos\alpha}{\cos\xi_3\cos\xi_4}, \tag{36}$$

$$N_q = \frac{g_2 g_4}{g_1 g_3}\cdot\frac{\tan\xi_3\tan\xi_4}{\tan\alpha}, \tag{37}$$

$$N_\gamma = \cos\alpha\left[\frac{g_2}{g_1}\cdot\frac{\cos\alpha\tan\xi_4}{\cos\xi_3} \times \left(\sin\xi_5 + \frac{g_4}{g_3}\cdot\frac{\sin\xi_3\tan\xi_4}{\tan\alpha}\right) - \sin\alpha\right], \tag{38}$$

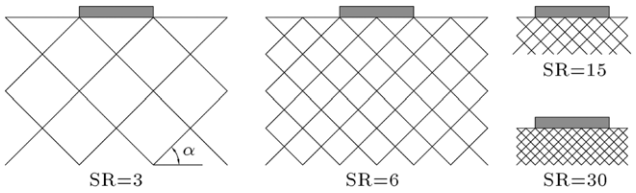

Figure 3: Strip footing on rock masses with two orthogonal joint sets, $\alpha = 45°$, $SR = 3$, 6, 15 and 30.

where:

$$g_1 = \cos\xi_1\sin\xi_2 - \sin 2\phi_j, \tag{39}$$

$$g_2 = \cos\xi_1 - \sin\xi_2\sin 2\phi_j, \tag{40}$$

$$g_3 = \sin 2\phi_j\cos\xi_2 + \sin\xi_1, \tag{41}$$

$$g_4 = \sin 2\phi_j + \cos\xi_2\sin\xi_1. \tag{42}$$

2.1.2. Failure mechanisms TS2 and OS2

It was not clear prior to the calculations, which mechanism would predict the minimum bearing capacity (optimum upper bound) for the jointed rock foundation. So, in addition to TS1 and OS1, the mechanisms TS2 and OS2 were also considered in order not to predefine the failure mechanism. For all cases analyzed, failure mechanisms TS1 and OS1 ensured the minimum limit load. For example, for the case of $\alpha = 45°$, $c_i = 5$ MPa $c_j = 50$ kPa, $\varphi_i = \varphi_j = 35°$, $q = 20$ kPa, $\gamma = 27$ kN/m^3 and $S_1 = S_2 = 3.9$ cm, the mechanism TS1 yields $n_0 = 100$ and $q_u = 210.8$ MPa, while the mechanism TS2 yields $n_0 = 101$ and $q_u = 572.3$ MPa. Therefore, the mechanisms TS2 and OS2 are not presented here.

2.2. Failure due to excessive deformation

Most of the existing analytical methods for determining ultimate bearing capacity of rock foundations are based on the general shear failure of the rock mass. Therefore, they do not seem to be proper for the case of a failure induced by excessive deformation of the mass. In such cases, load–settlement curve is a popular tool in estimating critical load. This curve can be obtained from loading tests in the field or using numerical methods, where the latter was used in this study by applying DEM. Jointed rock foundations containing two orthogonal joint sets were considered for dealing with the problem of failure due to excessive deformation. Figure 3 shows the general configuration of some of the constructed models for $\alpha = 45°$.

In the case of failure due to excessive deformation, no marked change in settlement is taken place in the load–settlement curve. In such cases, the stress corresponding to a settlement equal to 10% of the foundation width is often defined as the bearing capacity (the 0.1B method). Maghous et al. [12] and Imani et al. [13] showed that this method may appropriately estimate the critical load of a rock foundation. Hence, this method was employed in the present study for determining the bearing capacity in the case of failure due to excessive deformation.

3. Results

3.1. General shear failure

The optimum upper bound bearing capacity is obtained by minimizing Eq. (20) with respect to the only unknown

$$q_{u,(TS1)} = \frac{2 \times (D_{BC} + D_{CD} + D_{BD} + D_{DE}) - W_{ABC} - 2 \times \left(W_{BCD} + W_{BDE} + W_q\right)}{B \cdot V_0} \tag{18}$$

Box III

$$q_{u,(OS1)} = \frac{D_{AC} + D_{BC} + D_{CD} + D_{BD} + D_{DE} - \left(W_{ABC} + W_{BCD} + W_{BDE} + W_q\right)}{B \cdot V_0 \cdot \cos\left(\alpha + \phi_j\right)} \tag{19}$$

Box IV

parameter, n_0. Two computer programs were prepared in MATLAB code to solve the bearing capacity equations for TS1 and OS1. The genetic algorithm provided in the code was used for minimization. The minimization procedure was performed subject to the following constraints for OS1:

$$\alpha + \theta < \frac{\pi}{2}, \quad 0 < \alpha + \theta - \phi_i - \phi_j < \frac{\pi}{2}, \quad n_0 > 0. \tag{43}$$

And for TS1, the constraint $0 < \alpha - \theta + \phi_i + \phi_j < \pi/2$ was applied in addition to the above constraints.

3.1.1. Comparison with other solutions

Figure 4 represents a comparison among the results of the proposed Upper Bound Solution (UBS) for the case of $SR = 50$, the numerical lower bound solution by Sutcliffe et al. [3] and the displacement finite element solution by Alehossein et al. [14]. The results are presented as q_u/c_i ratio versus α for the case of a footing resting on the surface of a weightless rock mass in which, $c_j/c_i = 0.1$ and $\varphi_i = \varphi_j = 35°$. As expected, the upper bound results are higher than the other two methods, especially higher than the results of the lower bound solution. As discussed previously, in the mechanisms TS1 and OS1, most of the velocity discontinuity lines passed through joint surfaces, the position of which was predefined. So, it was not possible to optimize their location and the minimization procedures of the mechanisms were performed only for one discontinuity line (CD). As a result, the differences between the results of the UBS and other methods were become large. Moreover, in the UBS, there is a jump between the q_u/c_i for $\alpha = 30°$ and $\alpha = 45°$, which is due to the conversion from the one-sided failure mechanism in $\alpha = 30°$ to the two-sided in $\alpha = 45°$. Moreover, in the proposed approach, when the value of "$\alpha + \theta - \varphi_i - \varphi_j$" (the angle between the velocity vectors $\mathbf{V}_1$ and $\mathbf{V}_{01}$ shown in Figure 2(a) and (b) becomes small, these velocity vectors become large, resulting in an increase in the bearing capacity. This phenomenon occurred for the properties assumed to obtain the bearing capacity in the case of $\alpha = 45°$.

3.1.2. Effect of joint spacing

Using the UBS, the effect of joint spacing was studied for the general shear failure. The cases examined here, include a footing resting on the surface of a rock mass, where both the weightless and ponderable rocks were considered. It should be noted that rock masses with different properties were analyzed by DEM and the displacement vectors obtained showed that the general shear failure occurs for all of the cases. The UBS was applied to investigate the effect of joint spacing in this regard.

For weightless rock masses, the q_u/c_i ratios versus SR are shown in Figures 5 and 6 for the rock mass properties depicted in the figures. As observed, SR value does not significantly affect bearing capacity.

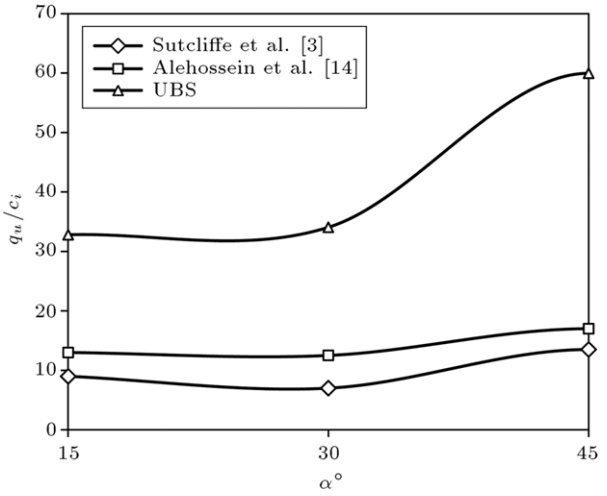

Figure 4: Comparison of q_u/c_i versus α obtained using Sutcliffe et al. [3] and Alehossein et al. [14] and the UBS.

For ponderable rock masses, Figures 7 and 8 show the q_u/c_i ratio versus SR for a ponderable rock mass with $\gamma = 27$ kN/m^3 and other properties depicted in the figures. SR value has also no pronounced effect on the bearing capacity in these cases.

3.1.3. Bearing capacity coefficients

Table 1 presents N_{cj}, N_{ci}, N_q and N_γ coefficients required for determining the ultimate bearing capacity of jointed rocks using the UBS (see Eq. (20)). According to the previous section, since the SR ratio does not have significant effect on the bearing capacity, it was assumed that $SR = 50$ in providing Table 1. This table can be used to determine the ultimate bearing capacity coefficients for practical cases.

3.2. Failure due to excessive deformation

Since in the case of failure due to excessive deformation, the shear surfaces in the material beneath the foundation do not reach the ground surface, the properties of the intact rock and the joint sets were selected such that the failure surfaces in the rock mass do not reach the ground surface. In the constructed numerical models, it was assumed that $\varphi_i = \varphi_j = 35°$, joint normal stiffness and joint shear stiffness (K_n and K_s, respectively) are equal to 100 GPa/m, $c_i = 20$ MPa and $c_j = 2$ MPa. Other specifications of the models were similar to those described previously for the selection of failure mechanisms for the case of general shear failure.

As an example, for the case of $\alpha = 45°$, Figures 9 and 10 show the settlement contours and the corresponding displacement vectors at a settlement equal to 10% of the footing width, for the case of SR values equal to 6 and 40, respectively. The

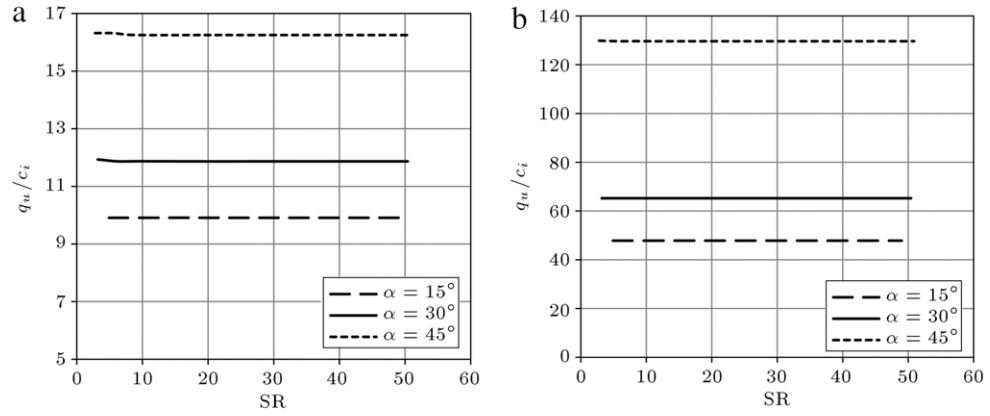

Figure 5: Variation of the q_u/c_i versus SR for the case of a weightless rock mass with $c_j/c_i = 0$ and (a) $\varphi_i = 35°$, $\varphi_j = 25°$ and (b) $\varphi_i = 45°$, $\varphi_j = 35°$.

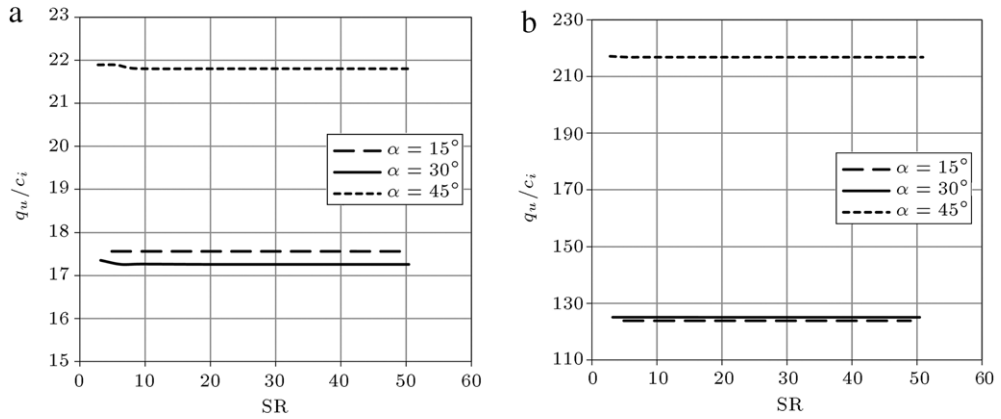

Figure 6: Variation of the q_u/c_i versus SR for the case of a weightless rock mass with $c_j/c_i = 0.1$ and (a) $\varphi_i = 35°$, $\varphi_j = 25°$ and (b) $\varphi_i = 45°$, $\varphi_j = 35°$.

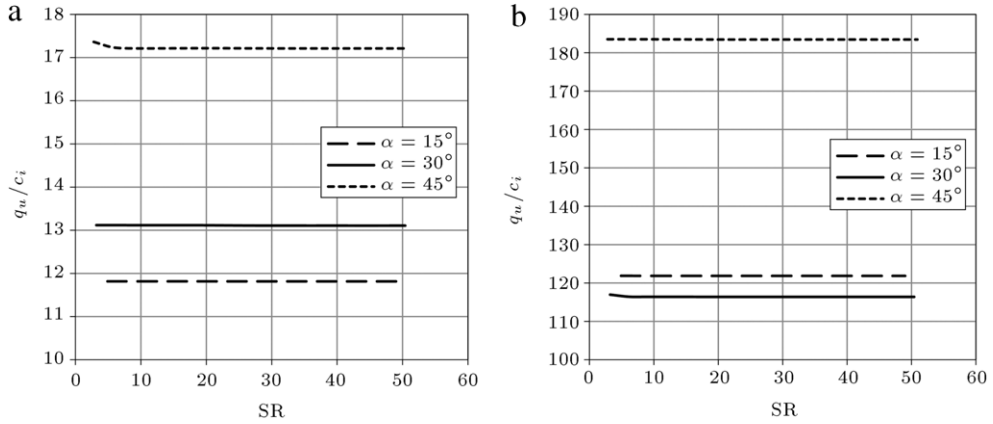

Figure 7: Variation of the q_u/c_i versus SR for the case of a ponderable rock mass with $c_j = 0$ and $c_i = 1$ MPa and (a) $\varphi_i = 35°$, $\varphi_j = 25°$ and (b) $\varphi_i = 45°$, $\varphi_j = 35°$.

displacement vectors are predominantly in the downward direction. Although few vectors are at an angle to the vertical, they do not show a flow pattern beneath the footing up to the ground surface. Therefore, it can be concluded that for the assumed properties of the intact rock and the joint sets, excessive deformation (settlement equal to 10% of the footing width) occurs prior to the general shear failure.

Figure 11 shows the variations of the q_u/c_i ratio obtained from the 0.1B method, versus SR for different values of α. According to the figure, for $SR < 30$, increasing the SR results in decreasing the bearing capacity, but for $SR > 30$, the joint spacing does not affect the bearing capacity significantly. Hence, $SR = 30$ can be taken into account as the approximate limit for the influence of jointing on the bearing capacity and it is named in this study as the critical spacing ratio (SR_{cr}).

DEM results are highly dependent on the selected rock parameters. For considering the effect of the intact rock and the joint set properties on the SR_{cr}, sensitivity analyses were performed. Because of the large number of models, the results of the case of $\alpha = 30°$ are only presented here. It should be noted that for all of the assumed properties for the intact rock and the joint sets in the following sections, excessive deformation

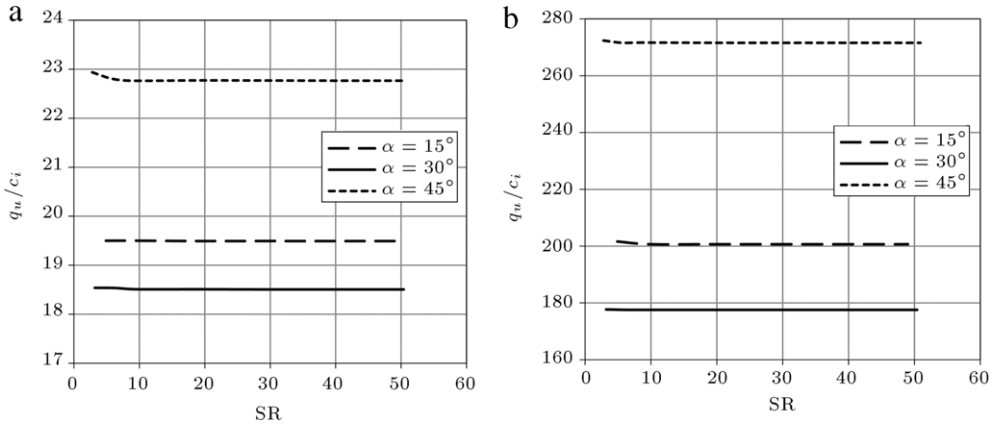

Figure 8: Variation of the q_u/c_i versus SR for the case of a ponderable rock mass with $c_j = 0.1$ MPa, $c_i = 1$ MPa and (a) $\varphi_i = 35°$, $\varphi_j = 25°$ and (b) $\varphi_i = 45°$, $\varphi_j = 35°$.

Table 1: Bearing capacity coefficients for jointed rock foundations.

$\alpha°$	$\varphi_i°$	$\varphi_j°$	N_{cj}	N_{ci}	N_q	N_γ
15	20	20	25.65	4.78	12.08	19.89
	30	20	41.17	6.75	19.88	43.26
		30	81.07	9.02	53.01	155.59
	40	20	74.39	10.47	36.86	110.23
		30	186.37	17.88	123.61	547.04
		35	351.63	24.10	267.44	1558.90
	50	20	168.74	19.69	85.88	387.66
		30	758.07	60.58	510.87	4452.54
		35	3237.01	185.2	2488.29	42,425.89
30	20	20	17.95	5.45	9.52	12.92
	30	20	28.08	7.68	15.65	28.42
		30	60.22	11.35	42.32	102.62
	40	20	49.45	11.91	28.99	72.63
		30	136.34	22.50	98.59	360.13
		35	275.92	32.60	221.56	1057.94
	50	20	109.39	22.37	67.48	253.92
		30	547.11	76.27	407.77	2908.24
		35	2523.5	251.26	2067.41	28,590.03
45	20	20	17.62	6.75	9.87	9.75
	30	20	26.73	9.51	16.22	21.44
		30	71.1	17.78	52.32	89.65
	40	20	45.72	14.73	30	54.26
		30	157.74	35.16	121.57	311.69
		35	399.63	64.06	334.57	1106.81
	50	20	98.23	27.59	69.64	187.09
		30	621.50	118.94	501.57	2477.09
		35	3620.92	494.36	3125.55	29,415.80

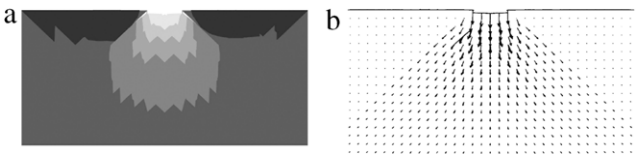

Figure 9: Rock mass with $\alpha = 45°$ and $SR = 6$. (a) Settlement contour, and (b) displacement vectors.

occurs in the rock mass and the displacement vectors of the rock blocks are similar to those presented in Figs. 9(b) and 10(b).

3.2.1. Effect of shear strength properties

Keeping c_i unchanged as it was assumed previously, Figure 12(a) shows the q_u/c_i versus SR for the case of $c_j/c_i = 0.1$, 0.3 and 0.5, while other properties of the rock mass are similar to those previously considered. Also, Figure 12(b) presents the q_u/c_i versus SR for $\varphi_i = \varphi_j = 25°$, 35° and 45° and other properties as they were assumed previously. The figures reveal that the $SR_{cr} = 30$ proposed in this research, does not change with changes in the c_j/c_i ratio if the deformation mode at critical load of the foundation remains unchanged.

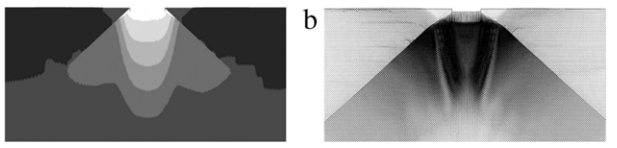

Figure 10: Rock mass with $\alpha = 45°$ and $SR = 40$. (a) Settlement contour and (b) displacement vectors.

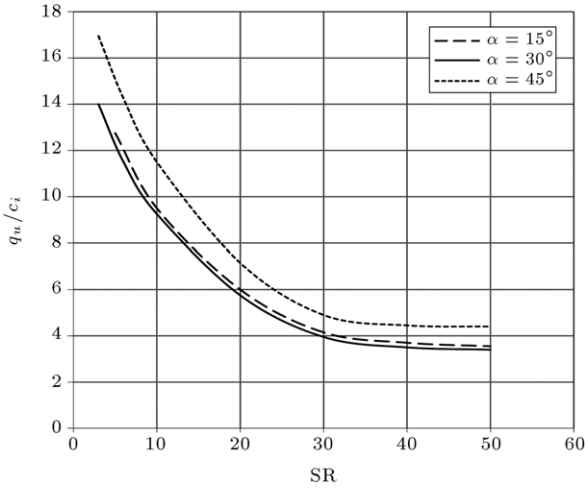

Figure 11: Variation of q_u/c_i with SR for two joint sets.

3.2.2. Effect of joint stiffness

To examine the influence of joint stiffness, analyses were performed using new joint normal stiffness and joint shear stiffness (K_{new}) equal to 25% and 50% smaller and larger than the initial values ($K_{ini} = 100$ GP/m) and the rest of the parameters were kept unchanged. According to Figure 13, it is clear that the stiffness of the joints does not change the SR_{cr}.

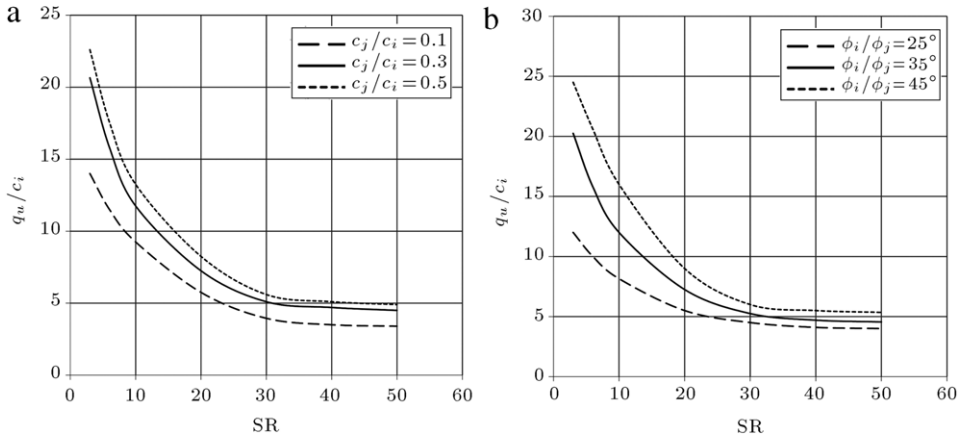

Figure 12: Variation of q_u/c_i versus SR for (a) $c_j/c_i = 0.1$, 0.3 and 0.5 and (b) $\varphi_i = \varphi_j = 25°$, 35° and 45°.

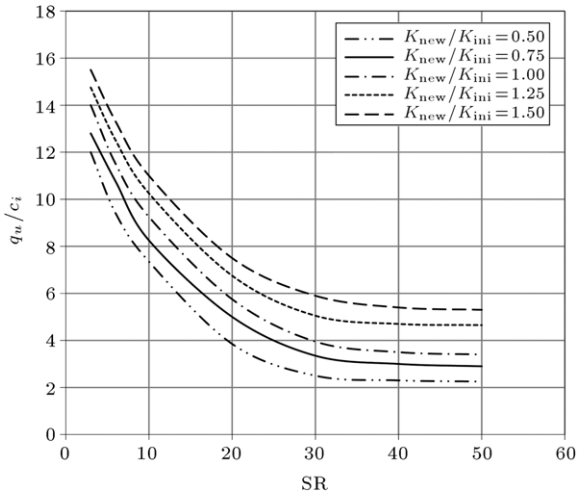

Figure 13: Effect of joint stiffness on the q_u/c_i versus SR.

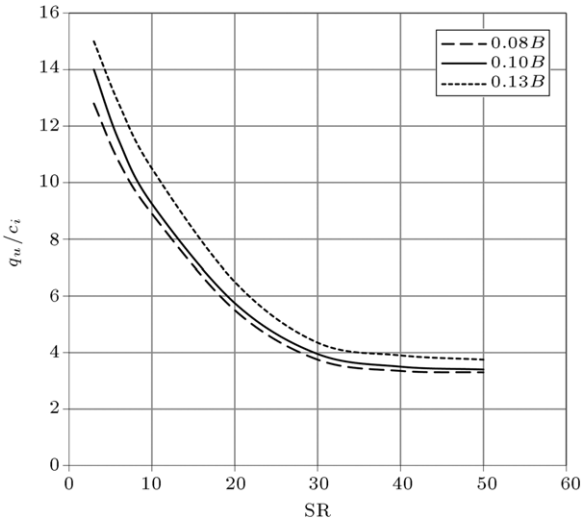

Figure 14: Effect of settlement limit on the q_u/c_i versus SR.

3.2.3. *Effect of settlement magnitude at critical load*

In this study, it is assumed that the excessive settlement that occurs at critical load of the rock mass is equal to 10% of the foundation width ($0.1B$). For investigating the effect of this hypothesis on the SR_{cr}, settlements equal to $0.08B$ and $0.13B$ were also examined and the rest of the parameters remained unchanged as they were assumed previously. Figure 14 reveals that the settlement limit does not have significant effect on the SR_{cr}.

3.2.4. *Effect of joint set numbers*

Analyses were performed for the rock foundations containing one and three joint sets. Additional models were also analyzed to investigate the influence of the number of the joint sets on the SR_{cr}, *the configuration of some of which is shown in* Figure 15. All of the intact rock and the joint sets properties were considered as previously. Figure 16(a) and (b) reveal that the SR_{cr} for both cases of one and three joint sets is similar to the condition of a rock foundation with two joint sets.

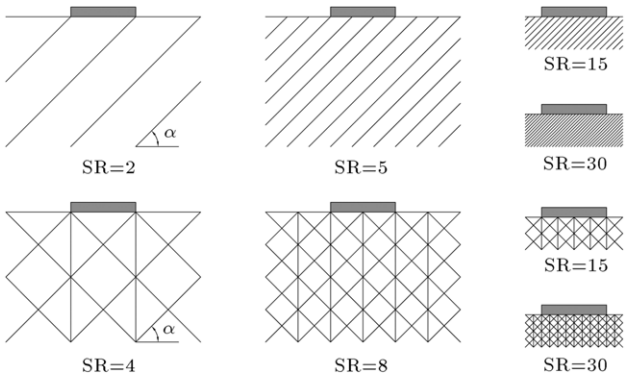

Figure 15: Strip footing on rock masses with one and three joint sets.

4. Discussions

Results of this study indicate that for the general shear failure, increase in c_i results in improving the contribution of intact rock cohesion in bearing capacity which tends to increase the q_u/c_i ratio. Increase in φ_i and φ_j leads to the greatest increment in bearing capacity in the case of $\alpha = 45°$, while the smallest for $\alpha = 15°$. This is because of the fact that by increasing the friction angles, the volume of failure mechanism for $\alpha = 45°$ becomes larger than the other orientations. The same results were also obtained for ponderable rocks. In this case, the contribution of the rock weight results in increasing the bearing capacity. Moreover, for

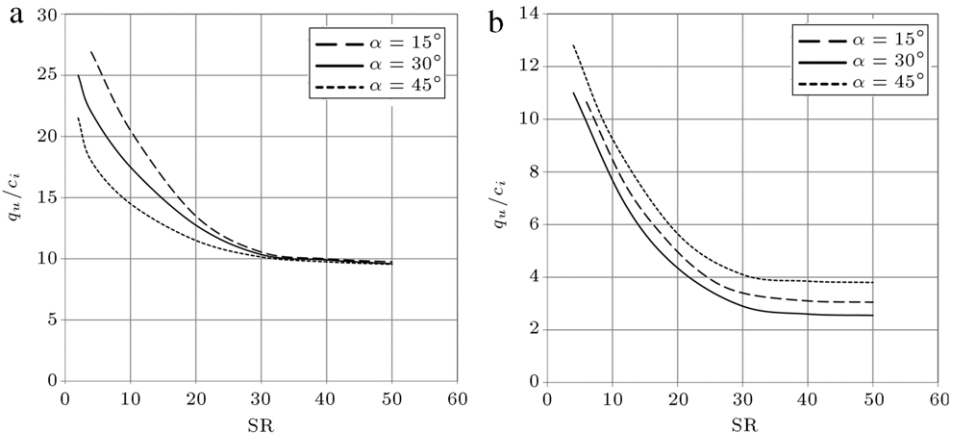

Figure 16: Variation of q_u/c_i versus SR for (a) one joint set and (b) three joint sets.

both weightless and ponderable rock masses, the SR ratio (and hence, the joint spacing) does not have remarkable effect on the bearing capacity. This conclusion is only valid for the cases in which the variations of joint spacing do not change the overall configuration of failure mechanism. In the UBS, as variation of SR imposes small changes in the location of discontinuity line CD, it does not change the overall configuration of the failure mechanisms. As discussed previously, for the rock models containing one through three joint sets, similar results were obtained by Halakatevakis and Sofianos [8].

The results obtained for the case of failure due to excessive deformation show that for $SR < 30$, increasing SR causes the q_u/c_i to decrease significantly. This is because of the fact that larger number of joints will provide smaller shear resistance because of the reduced roughness of the rock mass. For $SR > 30$, the rate of reduction in q_u/c_i, decreases remarkably, which implies that the reduction of joint spacing does not affect the bearing capacity any more. Also, the difference in the q_u/c_i ratios for various orientation angles decreases for the case of $SR > 30$ which means the small effect of joint spacing on the bearing capacity for $SR > 30$. The sensitivity analyses performed in this study shows that the mechanical properties of the rock mass do not significantly affect the influence of SR on the bearing capacity for the case of failure due to excessive deformation.

Hence, one can say that in the case of general shear failure, the effect of joint spacing on the bearing capacity is negligible. But in the failure due to excessive deformation, reduction in joint spacing results in reduction of bearing capacity for $SR < 30$, while it does not have significant effect in the case of $SR > 30$.

5. Conclusions

Two main bearing failure modes of jointed rock foundations were discussed in this study and the effect of joint spacing were investigated in each case. It was concluded that in the case of general shear failure, the joints spacing do not change the bearing capacity of the assumed jointed rock foundations significantly, while the bearing capacity will be affected when the failure is due to excessive deformation of the rock foundation. In the recent case, for $SR < 30$, increasing the SR results in decreasing the bearing capacity, but for $SR > 30$, the joint spacing does not significantly affect the bearing capacity.

Since the failure, due to excessive deformation, may occur prior to the general shear failure, determining the ultimate bearing capacity of rock foundations only by using the equations based on the general shear failure of rock foundation, may lead to unrealistic results. Therefore, in practical applications, allowable bearing capacity could be determined using the following procedure:

1. Determination of the ultimate bearing capacity using the methods based on general shear failure of the rock mass (like the UBS) and applying an appropriate safety factor.
2. Determination of the ultimate bearing capacity using the methods which are capable of taking into account the failure induced by excessive deformation (like DEM), and applying an appropriate safety factor.
3. Determination of the foundation pressure pertinent to the allowable settlement.
4. Using possibly the minimum value obtained from the three above stages as the final allowable bearing capacity.

In proceeding to the second stage mentioned above, the $SR_{cr} = 30$ proposed in this study is a very useful criterion. It shows that even for a jointed rock mass with $SR > 30$, the ultimate bearing capacity cannot be further decreased for the SR ratios greater than 30.

For dealing with the effect of joint spacing on the bearing capacity, specific properties were assumed for the rock mass in order to form the general shear failure for some cases and failure due to excessive settlement for other cases. Numerical analyses were carried out to determine the possible failure mode; however, because of great varieties in the properties of rock masses, using numerical analyses may not be possible for practical applications. Therefore, it would be better to derive simple charts or tables in this regard. For achieving this purpose, an extensive field test seems to be necessary.

References

[1] Serrano, A. and Olalla, C. "Ultimate bearing capacity of an anisotropic discontinuous rock mass, part I: basic modes of failure", *Int. J. Rock Mech. Min. Sci.*, 35(3), pp. 301–324 (1998).
[2] Serrano, A. and Olalla, C. "Ultimate bearing capacity of an anisotropic discontinuous rock mass, part II: determination procedure", *Int. J. Rock Mech. Min. Sci.*, 35(3), pp. 325–348 (1998).
[3] Sutcliffe, D.J., Yu, H.S. and Sloan, S.W. "Lower bound solutions for bearing capacity of jointed rock", *Comput. Geotech.*, 31, pp. 23–36 (2004).
[4] Yang, X.L. and Yin, J.H. "Upper bound solution for ultimate bearing capacity with a modified Hoek–Brown failure criterion", *Int. J. Rock Mech. Min. Sci.*, 42, pp. 550–560 (2005).

[5] Merifield, R.S., Lyamin, A.V. and Sloan, S.W. "Limit analysis solutions for the bearing capacity of rock masses using the generalised Hoek–Brown criterion", *Int. J. Rock Mech. Min. Sci.*, 43, pp. 920–937 (2006).
[6] Saada, Z., Maghous, S. and Garnier, D. "Bearing capacity of shallow foundations on rocks obeying a modified Hoek–Brown failure criterion", *Comput. Geotech.*, 35, pp. 144–154 (2008).
[7] Maghous, S., de Buhan, P. and Bekaert, A. "Failure design of jointed rock structures by means of a homogenization approach", *Mech. Cohesive Frict. Mater.*, 3, pp. 207–228 (1998).
[8] Halakatevakis, N. and Sofianos, A.I. "Strength of a blocky rock mass based on an extended plane of weakness theory", *Int. J. Rock Mech. Min. Sci.*, 47, pp. 568–582 (2010).
[9] Serrano, A. and Olalla, C. "Allowable bearing capacity of rock foundations using a non-linear failure criterium", *Int. J. Rock Mech. Min. Sci. Geomech. Abstr.*, 33, pp. 327–345 (1996).
[10] Frank, R., Bauduin, C., Driscoll, R., Kavvadas, M., Ovesen, N.K., Orr, T. and Schuppener, B., *Designer's Guide to EN 1997-1, Eurocode 7: Geotechnical Design-General Rules*, first ed., Thomas Telford, London (2004).
[11] Davis, E.H. "Theories of plasticity and the failure of the soil masses", In *Soil Mechanics: Selected Topics*, I.K. Lee, Ed., Butterworths, London (1968).
[12] Maghous, S., Bernaud, D., Freard, J. and Garnier, D. "Elastoplastic behavior of jointed rock masses as homogenized media and finite element analysis", *Int. J. Rock Mech. Min. Sci.*, 45, pp. 1273–1286 (2008).
[13] Imani, M., Sharifzadeh, M., Fahimifar, A. and Haghparast, P. "A characteristic criterion to distinguish continuity of rock masses applicable to foundations", *Proc. 45th US Rock Mech/ Geomech. Symposium*, San Francisco, USA, ARMA-11-508 (2011).
[14] Alehossein, H., Carter, J.P. and Booker, J.R. "Finite element analysis of rigid footings on jointed rock", *Proc. 3rd Int. Conf. Computational Plasticit*, 2, pp. 935–945 (1992).

Meysam Imani obtained his B.S. in civil engineering from Tehran University in 2004. He received his M.Sc. and Ph.D. degrees in soil mechanics and foundation engineering from Amirkabir University of Technology (Tehran Polytechnic) in 2006 and 2012, respectively. He published several papers in the field of rock foundations in different journals and international conferences. He has delivered some lectures on Soil Mechanics and Foundation Engineering in Amirkabir University of Technology, Garmsar Campus and also in Islamic Azad University. The main topics of his research interests are: Analytical Methods in Geomechanics, Upper and Lower Bound Methods of Limit Analysis, Rock Foundations, Finite Element Modeling of Soil–Structure Interaction and Mechanized Tunneling. He has also made contributions as a geotechnical consultant in practical projects such as Mechanized Tunneling, Concrete Dams and Cement Factories.

Ahmad Fahimifar studied civil engineering at Iran University of Science and Technology, gaining B.S. degree in 1976. After a period in industry, he continued his M.S. in the University of Birmingham (United Kingdom). He was awarded a Ph.D. degree by the University of Newcastle Upon Tyne (United Kingdom) in 1990 for his work on behavior of jointed rocks.

He began his academic activities in the Department of Civil Engineering at Amirkabir University of Technology in 1990, and appointed as the Head of Department in 1992. He has delivered many lectures on Rock Mechanics and Tunnel Engineering. In 2006 he was appointed as Professor at Amirkabir University. He is a member of International Society for Rock Mechanics, the founder and a member of Iranian Society for Rock Mechanics, the founder and a member of Iran Tunneling Association, and the founder and a member of Iranian Society of Civil Engineers. He is a member of some Iranian research journals including: Amirkabir Journal of Science and Technology, ASAS Journal of Civil Engineering, and Journal of Engineering Geology and the Environment.

Mostafa Sharifzadeh has a B.S. degree in Mining Engineering (1993-Kerman University), an M.S. degree in Engineering Rock Mechanics (1997-Amirkabir University of Technology, Tehran, Iran), and a Ph.D. degree in Environmental Geotechnology (2005-Kyushu University, Japan). Currently he is Associate Professor in Amirkabir University of Technology (Tehran Polytechnic). He is the author of papers on various subjects in rock mechanics, rock engineering, geotechnical engineering, tunnel engineering and numerical modeling. He has published over 200 publications including 3 books, 35 national and international indexed journal paper, and 100 conference papers in national and international conferences, 25 reports, 45 guideline and standards. He has successfully supervised over 20 undergraduate and 45 graduate students' thesis in master and doctoral level.